

# STUDY OF THE REACTION $np \rightarrow np\pi^+\pi^-$ AT INTERMEDIATE ENERGIES

A.P. Jerusalimov, Yu.A.Troyan, A.Yu.Troyan, A.V.Belyaev, E.B.Plekhanov  
JINR, Dubna, Moscow region, 141980, Russia

## Abstract

The reaction  $np \rightarrow np\pi^+\pi^-$  was studied at the various momenta of incident neutrons. It was shown that the characteristics of the reaction at the momenta above 3 GeV/c could be described by the model of reggeized  $\pi$  exchange (OPER). At the momenta below 3 GeV/c, it was necessary to use additionally the mechanism of one baryon exchange (OBE).

## 1 Introduction: study of inelastic np interactions at accelerator facility of LHEP JINR

The data about inelastic np interactions were obtained due to irradiation of 1m hydrogen bubble chamber ( $4\pi$  geometry) by quasimonochromatic neutron beam ( $\delta P < 2.5\%$ ) at the following incident momenta:

$P_0=1.25, 1.43, 1.73, 2.23, 3.10, 3.83, 4.10$  and  $5.20$  GeV/c

The unique of fullness and precision data are obtained [1]. It permits to carry out the detailed study of inelastic  $np$  interactions in a wide region of energies.

## 2 The reaction $np \rightarrow np\pi^+\pi^-$ at $P_0 > 3$ GeV/c

This reaction is characterized by:

- plentiful production of the  $\Delta$ -resonance (see Fig.2),
- large peripherality of the secondary nucleons.

To study the mechanism of the reaction it was chosen the model of reggeized  $\pi$  exchange (OPER), developed in ITEP [2].

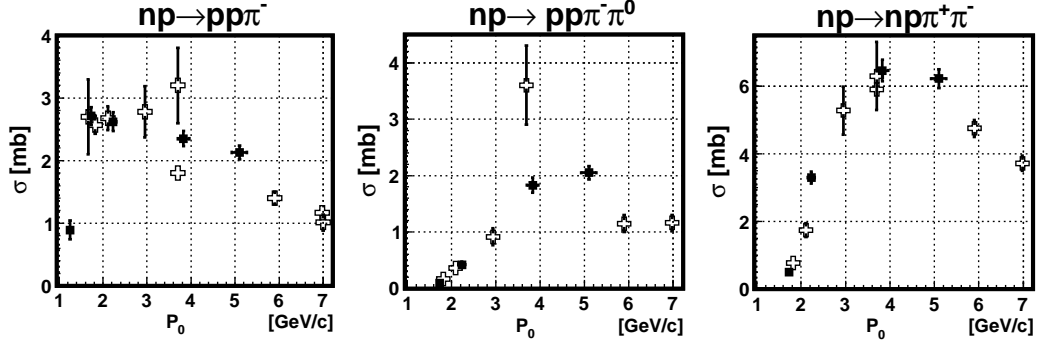


Figure 1: Cross-sections of some inelastic  $np$  interactions (black squares - our data)

The advantages of OPER model are:

- small number of free parameters (3 in our case),
- wide region of the described energies (2÷200 GeV),
- calculated values are automatically normalized to the reaction cross-section.

The following main diagrams correspond to the reaction  $np \rightarrow np\pi^+\pi^-$  within the framework of OPER model:

Matrix element for the diagrams a, b and c from Fig. 3 is written in the following form:

$$M_1 = T_{\pi N \rightarrow \pi N} F_2 T_{\pi N \rightarrow \pi N} / (t - m_\pi^2),$$

where  $T_{\pi N \rightarrow \pi N}$  - amplitude of elastic  $\pi N \rightarrow \pi N$  scattering off mass shell,

$F_2$  - form-factor, going away off mass shell of  $T_{\pi N \rightarrow \pi N}$  amplitudes,

$1/(t - m_\pi^2)$  -  $\pi$ -meson propagator.

The data of elastic  $\pi N \rightarrow \pi N$  were taken from PWA [3].

The analysis shows, that interference between diagrams 3a ,3b and 3c is negligible [4].

The study has shown that it is not necessary to take into account the contribution of the "hanged" diagrams (Fig.) into the reaction cross-sections at  $P_0 < 10$  GeV/:

It was shown in [5] that the use of some specific cuts permits to select the kinematic region of the reaction  $np \rightarrow np\pi^+\pi^-$  in which the contribution of the diagrams 3a, 3b and 3c consists up to 95 % at  $P_0 > 3$  GeV/c.

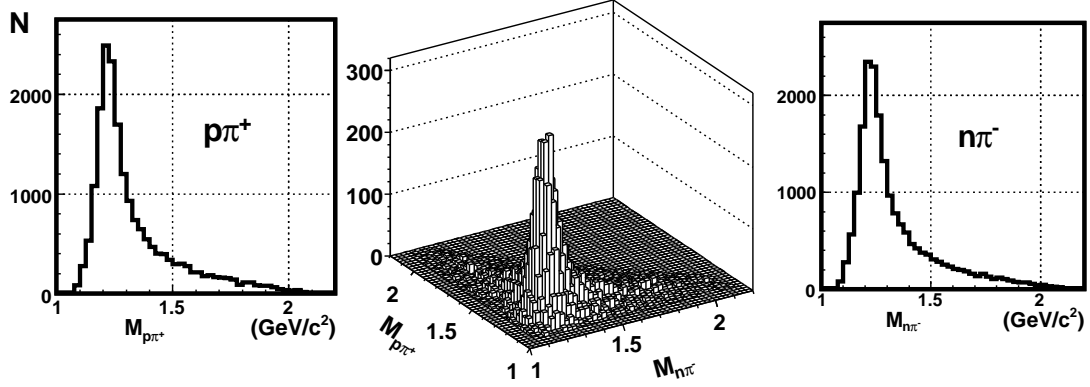


Figure 2: The distributions of  $M_{p\pi^+}$  and  $M_{n\pi^-}$  from the reaction  $np \rightarrow np\pi^+\pi^-$  at  $P_0 = 3 \text{ GeV}/c$

Fig.5 shows some distributions for the reaction  $np \rightarrow np\pi^+\pi^-$  for this region at  $P_0=5.20 \text{ GeV}/c$  (solid curves - results of calculations using OPER model).

But the diagrams shown in Fig.3 are insufficient to describe totally the characteristics of the reaction  $np \rightarrow np\pi^+\pi^-$ . It is necessary to take into account the diagrams of the following type:

the matrix element for which is written in the following form:

$$M_3 = G\bar{u}(q_N)\gamma_5 u(Q_N)F_1 T_{\pi N \rightarrow \pi\pi N} / (t - m_\pi^2),$$

where  $T_{\pi N \rightarrow \pi\pi N}$  - off mass shell amplitudes of inelastic  $\pi N \rightarrow \pi\pi N$  - scattering that are known much worse than elastic  $T_{\pi N \rightarrow \pi N}$  amplitudes. Therefore it is necessary to do a parametrization of the inelastic  $\pi N \rightarrow \pi\pi N$ -scattering (see Appendix).

It permits to get a good description of the experimental characteristics of the reaction  $np \rightarrow np\pi^+\pi^-$  at  $P_0=5.20 \text{ GeV}/c$  (Fig.7) taking into account OPER diagrams shown in Fig.3 and Fig.6 :

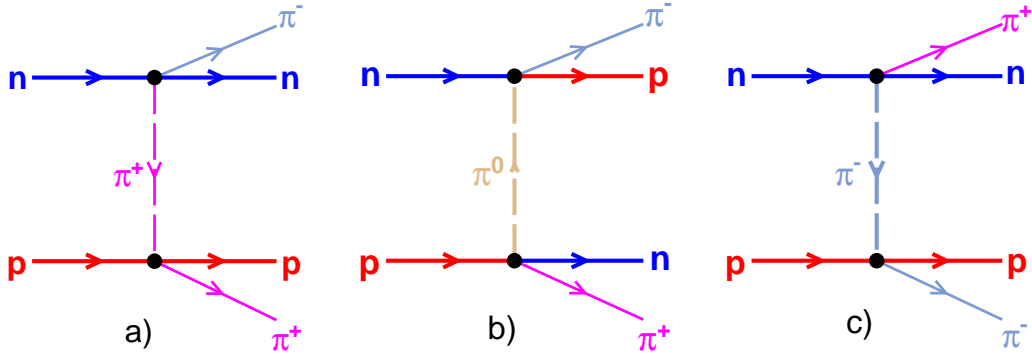


Figure 3: OPER diagrams  $2 \times 2$  for the reaction  $np \rightarrow np\pi^+\pi^-$

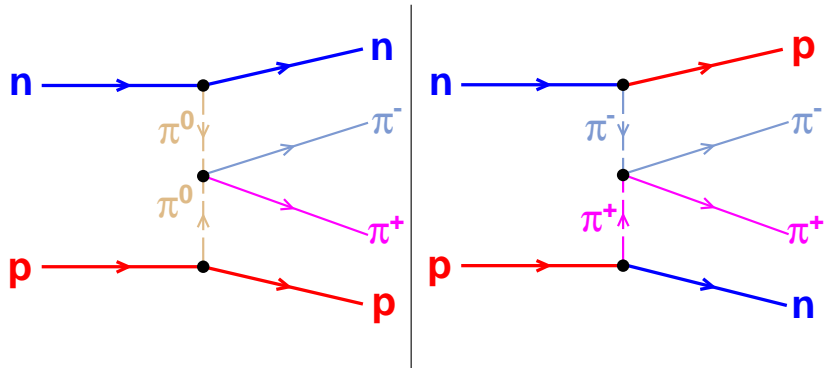


Figure 4: "Hanged" OPER diagram for the reaction  $np \rightarrow np\pi^+\pi^-$

### 3 The reaction $\bar{p}p \rightarrow \bar{p}p\pi^+\pi^-$ at $P_0 = 7.23$ GeV/c

Using OPER model we try to describe the experimental distributions from the reaction  $\bar{p}p \rightarrow \bar{p}p\pi^+\pi^-$  at  $P_0 = 7.23$  GeV/c [5]

It is observed a good agreement between experimental data and theory in Fig.8.

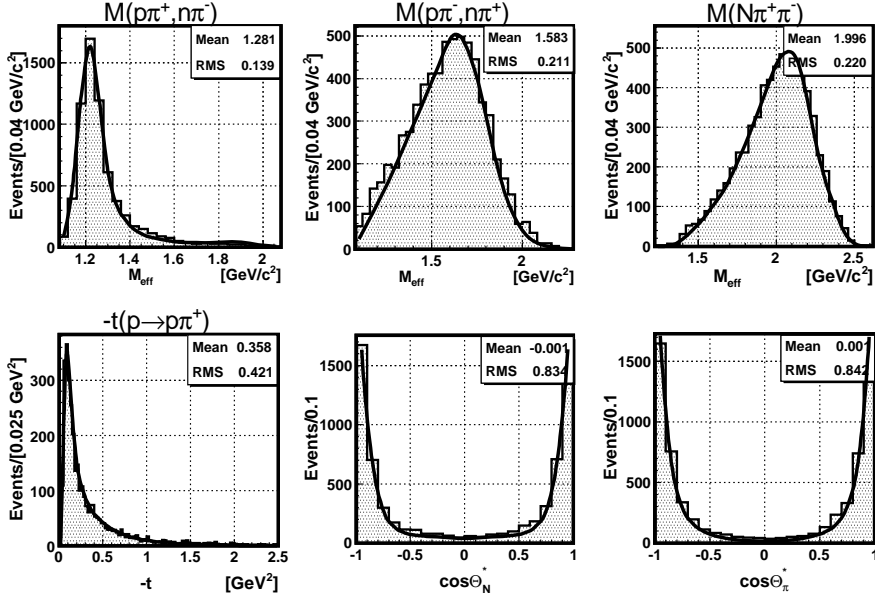


Figure 5: Distributions for the reaction  $np \rightarrow np\pi^+\pi^-$  at  $P_0=5.20$  GeV/c obtained due to specific cuts.

#### 4 The reaction $np \rightarrow np\pi^+\pi^-$ at $P_0 < 3$ GeV/c

The study of effective mass spectra of  $np$  - combinations at  $P_0=1.73$  and 2.23 GeV/c (Fig.9) shows the clear peak close the threshold ( $M_{np} = m_n + m_p$ ) that can not be described within the framework of OPER-model using the diagrams from Fig.3 and Fig.6.

The model of Regge poles with baryon exchange and nonlinear trajectories, suggested in [6] was used to describe these features. The following diagrams of one baryon exchange (OBE) were taken into account within the framework of this model:

The vertex function of elastic  $np \rightarrow np$  scattering was calculated using the data from [7].

The vertex functions of  $\Delta N \rightarrow np$ ,  $NN \rightarrow \Delta N$  and  $\Delta N \rightarrow \Delta N$  scattering were calculated corresponding to [8]. In result one can get the good description of the experimental distribution from the reaction  $np \rightarrow np\pi^+\pi^-$  at  $P_0 = 1.73$  and 2.23 GeV/c (Fig.9 and Fig.11).

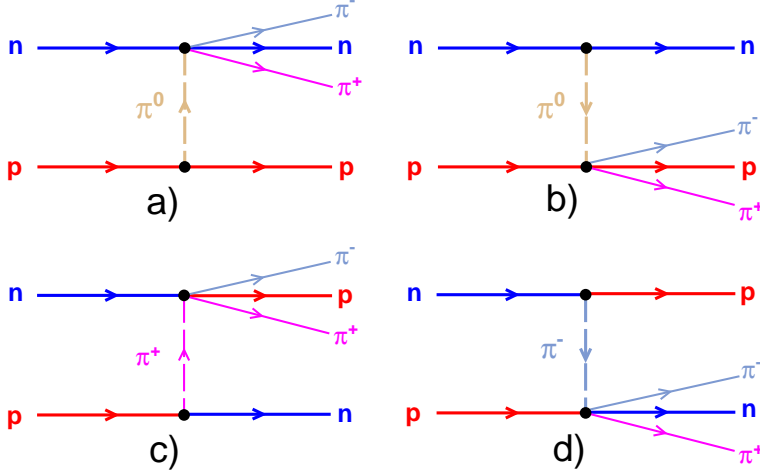


Figure 6: OPER diagrams  $1 \times 3$  for the reaction  $np \rightarrow np\pi^+\pi^-$

## 5 OPER model and other reactions

The other reactions of np interactions are scheduled to study by means of OPER model:

$np \rightarrow pp\pi^-$	vertex functions $1 \times 2$
$np \rightarrow pp\pi^-\pi^0$	vertex functions $2 \times 2$ and $1 \times 3$
$np \rightarrow pp\pi^+\pi^-\pi^-$	vertex functions $2 \times 3$
$np \rightarrow pp\pi^+\pi^-\pi^-\pi^0$	vertex functions $3 \times 3$
$np \rightarrow np\pi^+\pi^-\pi^+\pi^-$	vertex functions $3 \times 3$

Similar reactions of  $pp$ ,  $\bar{p}p$  and  $\pi N$  interactions also can be described by OPER model. The following reactions were simulated for HADES experiment:

$$\begin{aligned}
 &pp \rightarrow pp\pi^+\pi^- \text{ at } T_{kin}=3.5 \text{ GeV} \\
 &np \rightarrow np\pi^+\pi^- \text{ at } T_{kin}=1.25 \text{ GeV} \\
 &np \rightarrow npe^+e^- \text{ at } T_{kin}=1.25 \text{ GeV} \text{ with vertex function of } \gamma N \rightarrow Ne + e^-.
 \end{aligned}$$

Since the  $\pi N \rightarrow \pi N$  and  $\pi N \rightarrow \pi\pi N$  vertex functions are taken in helicity representation it seems to be perspective to use OPER model for description of the reaction with polarized particles.

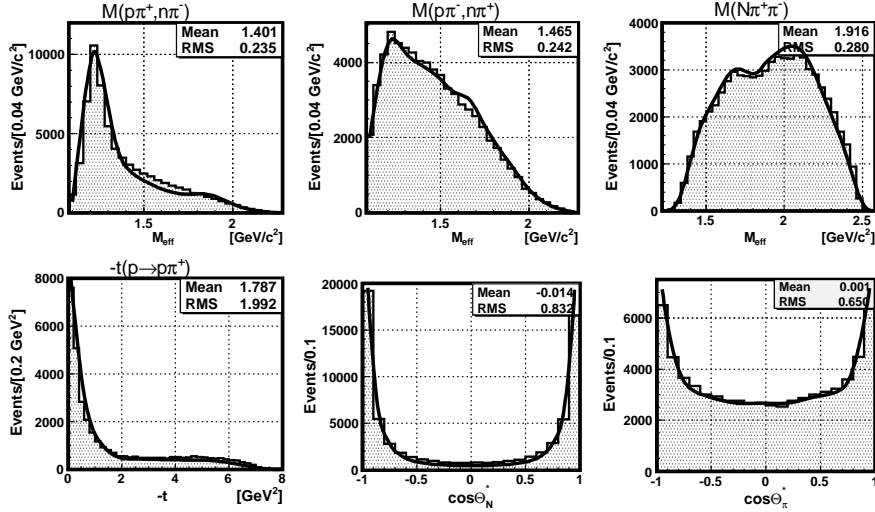


Figure 7: Distributions for the reaction  $np \rightarrow np\pi^+\pi^-$  at  $P_0=5.20$  GeV/c

## 6 Conclusion

Reaction  $np \rightarrow np\pi^+\pi^-$  is characterized by the plentiful production of the  $\Delta$  resonance and the large peripherality of the secondary particles. The experimental data are successfully described by the further development of OPER model.

However at  $P_0 < 3$  GeV/c it is necessary to take into account another mechanism of the reaction (such as OBE).

OPER model permits to describe another  $N(\bar{N}) - N$  reactions with the production of some  $\pi$ -mesons. The further development of OPER-model can be very promising to describe the production of  $e^+e^-$ -pairs in hadronic interactions.

OPER model can be used as an effective tool to simulate various reactions of hadronic interactions.

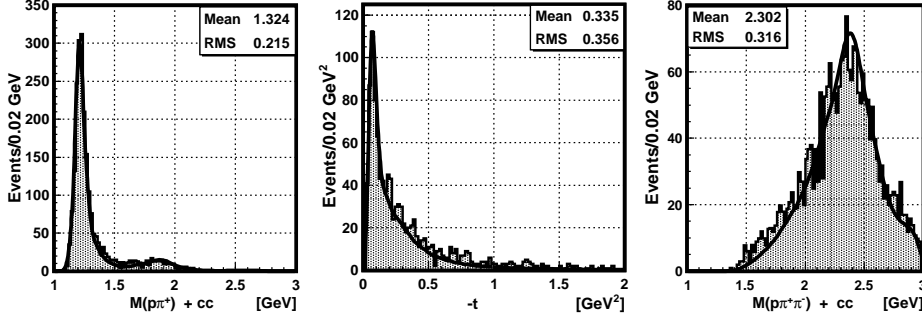


Figure 8: Distributions for the reaction  $\bar{p}p \rightarrow \bar{p}p\pi^+\pi^-$  at  $P_0 = 7.23$  GeV/c

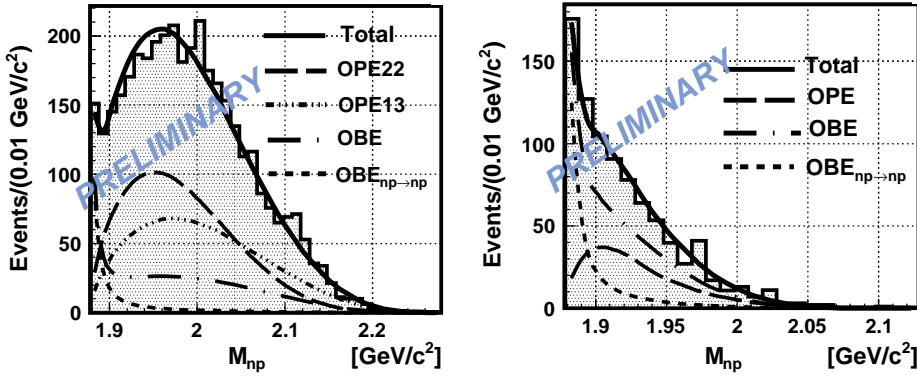


Figure 9: The distributions of  $M_{np}$  for treaction  $np \rightarrow np\pi^+\pi^-$  at  $P_0 = 2.23$  GeV/c (left) and 1.73 GeV/c (right).

## 7 Appendix: Parametrization of $\pi N \rightarrow \pi\pi N$ reactions

Within the framework of Generalized Isobar Model (GIM) [9]  $\pi N \rightarrow \pi\pi N$  reactions are described as quasi-two body ones ( $a + b \rightarrow c + d$ ):

$$\begin{aligned} \pi N &\rightarrow N^*(\Delta^*) \rightarrow \Delta\pi, \\ \pi N &\rightarrow N^*(\Delta^*) \rightarrow N\rho \\ \pi N &\rightarrow N^*(\Delta^*) \rightarrow N\epsilon \\ \pi N &\rightarrow N^*(\Delta^*) \rightarrow N_{1440}^*\pi \end{aligned}$$

with the consequent decays:

$$\Delta \rightarrow N\pi,$$



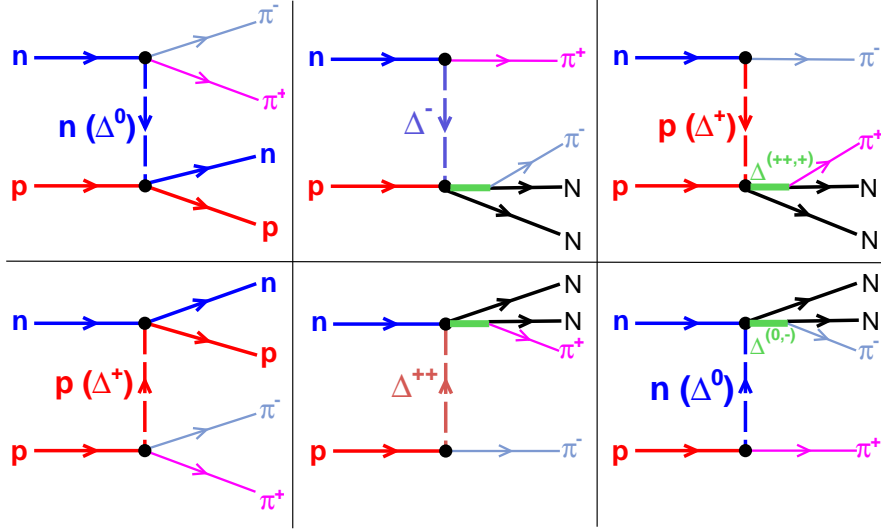


Figure 10: OBE diagrams for the reaction  $np \rightarrow np\pi^+\pi^-$

$$\begin{aligned}
 \rho &\rightarrow \pi\pi, \\
 \rho &\rightarrow \pi\pi, \\
 N_{1440}^* &\rightarrow N\pi
 \end{aligned}$$

The parameters of the following resonances (\*\*\*\* and \*\*\*) were taken from Review of Particle Properties:

$$\begin{array}{ll}
 N^*(1440)P11 & D^*(1600)P33 \\
 N^*(1520)D13 & D^*(1620)S31 \\
 N^*(1675)D15 & D^*(1700)D33 \\
 N^*(1680)F15 & D^*(1900)S31 \\
 N^*(1720)P13 & D^*(1905)F35 \\
 N^*(2000)F15 & D^*(1910)P31 \\
 N^*(2080)D13 & D^*(1920)P33 \\
 N^*(2190)G17 & D^*(1940)D33 \\
 & D^*(1950)F37
 \end{array}$$

The spin and isospin relations were taken account.

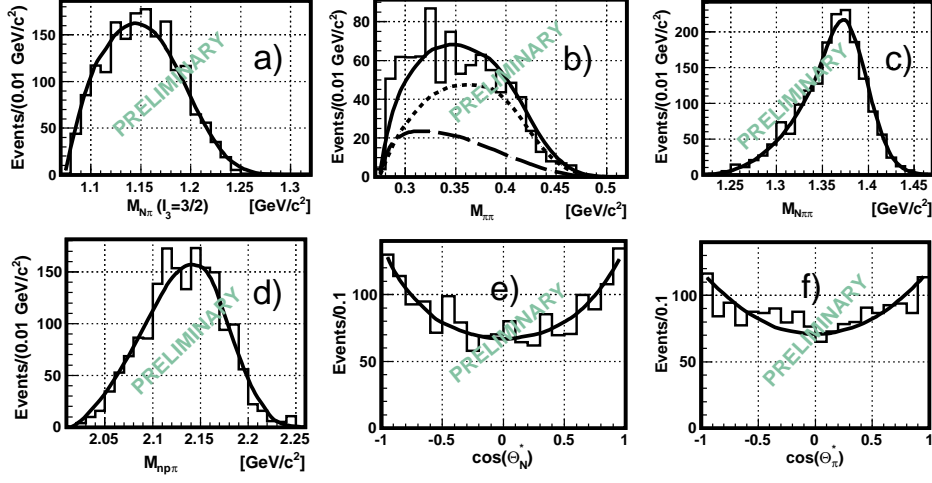


Figure 11: Distributions for the reaction  $np \rightarrow np\pi^+\pi^-$  at  $P_0=1.73$  GeV/c

For quasi two-body reactions like  $a + b \rightarrow c + d$  one can write

$$d\sigma = \frac{1}{(2S_a + 1)(2S_b + 1)} \left( \frac{2\pi}{p} \right)^2 \sum_{\lambda_i} | \langle \lambda_d \lambda_c | T | \lambda_b \lambda_a \rangle |^2 \times dPS ,$$

$$\langle \lambda_d \lambda_c | T | \lambda_b \lambda_a \rangle = \frac{1}{4\pi} \sum_j (2j + 1) \langle \lambda_d \lambda_c | T_j | \lambda_b \lambda_a \rangle e^{i(\lambda - \mu)\varphi} d_{\lambda\mu}^j(\theta) .$$

where  $\lambda = \lambda_a - \lambda_b$ ,  $\mu = \lambda_c - \lambda_d$  - helicity variables,

$d_{\lambda\mu}^j(\theta)$  - rotation matrix,

$dPS$  - phase space element.

The polarization components of the particles  $c$  and  $d$  from the reaction  $a + b \rightarrow c + d$  is suitable to express through the elements of the spin density matrix (for example, for particle  $d$ ):

$$\rho_{mm'}^d = \frac{1}{N} \sum_{\lambda_c \lambda_b \lambda_a} \langle m \lambda_c | T | \lambda_b \lambda_a \rangle^* \langle m \lambda_c | T | \lambda_b \lambda_a \rangle$$

where normalization factor for  $\text{Sp}\rho=1$ :

$$N = \sum_{m \lambda_c \lambda_b \lambda_a} \langle m \lambda_c | T | \lambda_b \lambda_a \rangle^2 .$$

### Example:

$$\pi + N \rightarrow N_{1680}^* \rightarrow \Delta + \pi \rightarrow (N + \pi) + \pi$$
$$\langle \lambda_{\Delta} | T | \lambda_N \rangle = C_{3,0;\frac{1}{2},-\lambda_{\Delta}}^{\frac{5}{2},-\lambda_N} C_{1,0;\frac{3}{2},-\lambda_{\Delta}}^{\frac{5}{2},-\lambda_{\Delta}} d_{-\lambda_N,-\lambda_{\Delta}}^{\frac{5}{2}}(\theta) \times R_J,$$

where  $R_J$  is taken in Breight-Wigner form.

Then it is easy to get the angular distribution of  $\Delta$  (in CMS):

$$\frac{d\sigma(s, t)}{d\Omega} \sim (1 + 2 \cos^2 \theta_{\Delta}) | R_J |^2 = (1 + 2 \cos^2 \theta_{\Delta}) \times BW(\sqrt{s}, M_R, \Gamma_R)$$

If particle d is unstable:  $d \rightarrow \alpha + \beta$  ( $d \rightarrow \Delta + \pi$ ) then in the rest system of the particle d:

$$W_{\Delta} = \frac{3}{4\pi} \left\{ \rho_{33} \sin^2 \theta + \frac{1}{3} \rho_{11} (1 + 3 \cos^2 \theta) - \frac{2}{\sqrt{3}} \text{Re} \rho_{3-1} \sin^2 \theta \cos 2\varphi - \frac{2}{\sqrt{3}} \text{Re} \rho_{31} \sin 2\theta \cos \varphi \right\}$$

- is the normalized angular distribution of the decay products.

To compare with experimental data the following cross-sections were calculated using GIM (Fig.12):

One can see a satisfactory description of cross-sections, except  $\pi^+ p \rightarrow n\pi^+\pi^+$ . May be it is necessary to take into account S-wave of  $\pi^+\pi^+$  scattering with I=2 in GIM.

Some distributions of the reaction  $\pi^- p \rightarrow n\pi^+\pi^-$  were calculated at various energies to study a quality of the application of GIM (Fig.13):

It is observed a good agreement between experimental data and theory.

## References

- [1] C.Besliu et al. YaF, 43:888-892,1986.

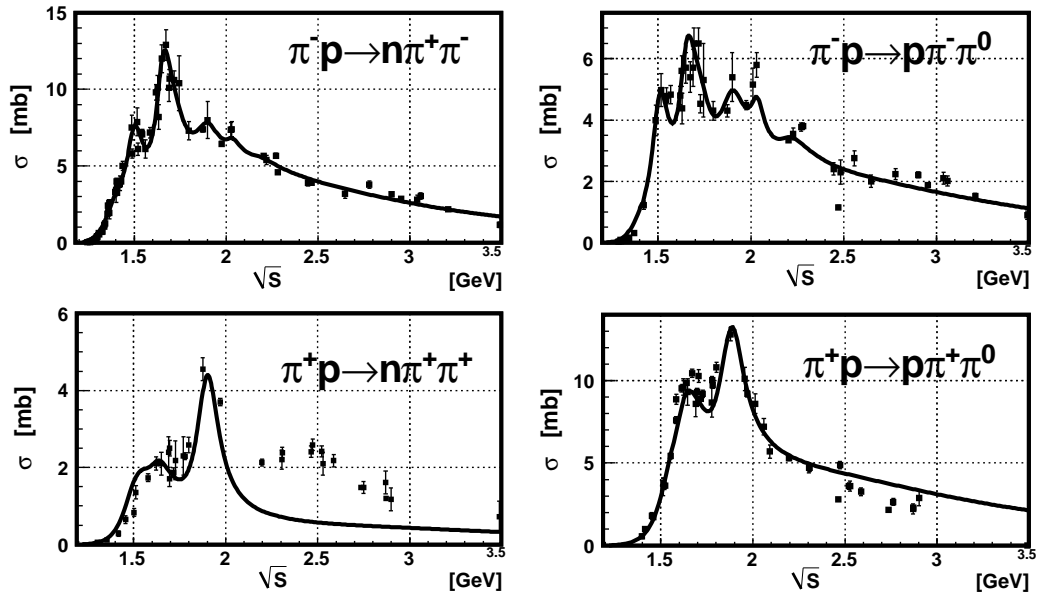


Figure 12: Cross-sections of the  $\pi n \rightarrow \pi \pi N$  reactions.

- [2] L.Ponomarev. Part. and Nucl., v.7(1), pp. 186-248, 1976, JINR, Dubna (in russian).
- [3] R.A. Arndt et al. IJMP A18(3), 2003, p. 449.
- [4] A.P.Jerusalimov et al. JINR Rapid Comm., v.35(2) pp.21-26, 1989, JINR, Dubna (in russian).
- [5] G.W. van Appeldorn et al, NP B156 (1979),pp. 110-125.
- [6] A.B. Kaydalov and A.F. Nilov. YaF, v.41(3),pp. 768-776, 1985 ;  
YaF, v.52(6), pp. 1683-1696, 1990.
- [7] NN and ND interactions - a compilation. UCRL-20000 NN, august 1970.
- [8] V.Barashenkov and B.Kostenko. JINR Comm. 4-84-761, 1984, JINR, Dubna.
- [9] D.J. Herndon et al. PR D11, 3165 (1975);  
D.M.Manley and E.M. Saleski, PR D45, 4002 (1992).
- [10] J.Dolbeau et al. NP B78, 233(1974).

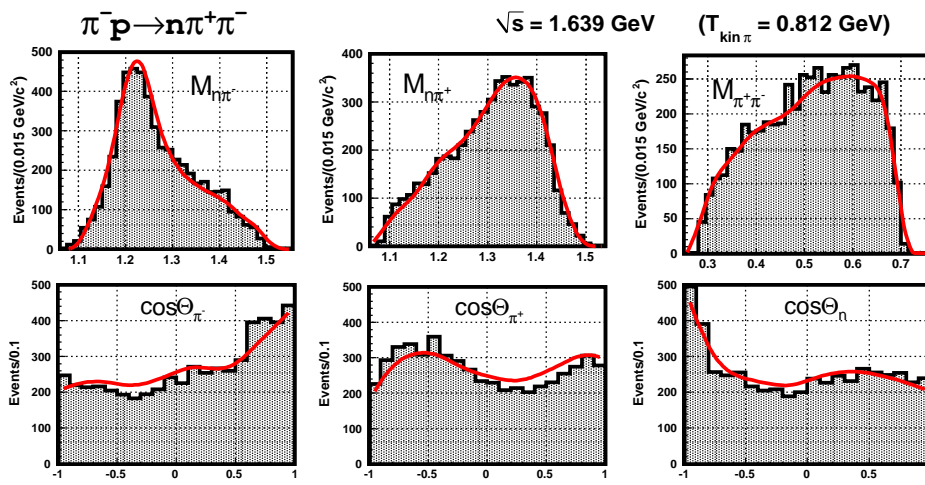


Figure 13: Some distributions from the reaction  $\pi^- p \rightarrow \pi^+ \pi^- n$  at  $T_{\text{kin}}=1.0 \text{ GeV}$  [10]